Generalized CC-TDSCF and LCSA: The system-energy representation

Sergio López-López, Mathias Nest and Rocco Martinazzo

View Online

Export Citation

ARTICLES YOU MAY BE INTERESTED IN

Generalized CC-TDSCF and LCSA: The system-energy representation

Sergio López-López,[1] Mathias Nest,[1] and Rocco Martinazzo[2,a]

[1]*Department of Theoretical Chemistry, Technische Universität München, Lichtenbergstraße 4, 85747 Garching, Germany*
[2]*Dipartimento di Chimica Fisica ed Elettrochimica and CIMAINA, Università di Milano, V. Golgi 19, 20133 Milan, Italy*

Typical (sub)system-bath quantum dynamical problems are often investigated by means of (approximate) reduced equations of motion. Wavepacket approaches to the dynamics of the whole system have gained momentum in recent years and there is hope that properly designed approximations to the wavefunction will allow one to correctly describe the subsystem evolution. The continuous-configuration time-dependent self-consistent field (CC-TDSCF) and local coherent-state approximation (LCSA) methods, for instance, use a simple Hartree product of bath single-particle-functions for each discrete variable representation (DVR) state introduced in the Hilbert space of the subsystem. Here we focus on the above two methods and replace the DVR states with the eigenstates of the subsystem Hamiltonian, i.e., we adopt an energy-local representation for the subsystem. We find that stable and semiquantitative results are obtained for a number of dissipative problems, at the same (small) computational cost of the original methods. Furthermore, we find that both methods give very similar results, thus suggesting that coherent-states are well suited to describe (local) bath states. As a whole, present results highlight the importance of the system basis-set in the selected-multiconfiguration expansion of the wavefunction. They suggest that accurate and yet computationally cheap methods may be simply obtained from CC-TDSCF/LCSA by letting the subsystem states be variationally optimized. © *2011 American Institute of Physics*. [doi:10.1063/1.3518418]

I. INTRODUCTION

System-bath dynamical problems are ubiquitous in chemical physics, where often a "subsystem" of interest can be identified, and possibly measured, while the environment is only partially under control. In such instances the role of the environment cannot be neglected since coupling to a heat bath may be needed to activate the system and/or to dissipate the excess energy of a reaction. In modeling these situations one often resorts to reduced dynamical methods, and the system dynamics is modified in such a way to account, at least approximately, for the influence of the bath. In the quantum case this procedure requires additional approximations if a manageable computational task is aimed at, but this comes at a price of a number of shortcomings. For instance, master equations as obtained from the theory of open quantum systems[1–3] hardly handle simultaneously medium and strong system-bath coupling, non-Markovian effects, nonlinearity and anharmonicity in the bath or subsystem-bath interaction, nonequilibrium states, initial correlation between the subsystem and bath, etc. An alternative approach, which consists in including the total subsystem+bath degrees of freedom (DOF) in the wavepacket dynamics, has attracted increasing attention in recent years. The resulting schemes are more flexible, less dependent on the specific form of the potentials—e.g., not restricted to Hamiltonians of the system-bath form—and free of the above-mentioned problems, but come at

a huge computational cost, due to the exponential scaling of current quantum dynamical methods. Enormous progress has been made in this respect, particularly with the multiconfiguration time-dependent Hartree (MCTDH) method.[4,5] MCTDH has opened the door to comparatively large systems, of tens of degrees of freedom, in a wide range of phenomena, such as photodissociation[6–9] and photoabsorption spectra,[10–12] predissociation,[13,14] and reactive[15–19] and molecule-surface scattering[20–25] (see Ref. 26 for an exhaustive list of MCTDH applications). MCTDH has also been applied to some system-bath dynamical problems,[27,28] but realistic systems still remain beyond current computational resources. Indeed, when simulating typical real processes by means of a finite-size bath, hundreds of bath DOF have to be included to make the Poincaré recurrence time larger than any time of interest for the subsystem dynamics.

Several methods have been developed to overcome the exponential scaling limitation. The standard MCTDH scheme has been extended to an exact, multilayer (ML) formulation[29–32] which enables the treatment of significantly larger and more complex systems, and a number of studies have been reported on system-bath problems, even at finite temperatures.[33] Though ML-MCTDH does not solve the basic exponential problem, it considerably enlarges the set of tractable systems and has been already used in molecular applications.[34–36] Among approximate schemes, those which partially replace the fully flexible single-particle functions with Gaussian functions—the so-called Gaussian-MCTDH (G-MCTDH) methods[37–39]—allow considerable

a)Electronic mail: rocco.martinazzo@unimi.it.

savings of both CPU time and random access memory by focusing attention on the most important degrees of freedom. The same is true for the coupled-coherent state method[40,41] which combines a coherent-state representation of the time-dependent Schrödinger equation with Monte Carlo sampling techniques. Alternatively, schemes such as the selected-MCTDH method[42] select and propagate only the most important configurations used for representing the wave function of the system. The continuous-configuration time-dependent self-consistent field (CC-TDSCF) scheme of Zhang *et al.*[43] follows a similar strategy and, within a system-bath picture, introduces approximations only in the bath description, while keeping a reasonably high level of accuracy for the subsystem dynamics.[44,45] Some of the present authors went further in approximating the CC-TDSCF wavefunction, and replaced the fully flexible single-particle functions of the bath with coherent states (CSs), thereby realizing what can be considered a selected-configuration G-MCTDH. The resulting method was called LCSA (Ref. 46) as it is based on a local coherent-state approximation to the system-bath dynamics. In this work we focus on LCSA and CC-TDSCF, and describe variants of these approaches. Notice that as CC-TDSCF results from a local, time-dependent Hartree approximation (LTDH) of the dynamics, in the following we use LTDH in place of CC-TDSCF to emphasize the relationship between the two methods.

LTDH and LCSA share the use of a discrete variable representation (DVR) to represent the state space of the system and of a Hartree product approximation for the resulting (local) bath states. Their *ansatz* takes the form

$$i\hbar|\Psi\rangle = \sum_{\alpha} C_{\alpha}|\xi_{\alpha}\rangle|\Phi_{\alpha}\rangle, \tag{1}$$

where $\{|\xi_{\alpha}\rangle\}$ is a DVR set for the subsystem coordinates, and $|\Phi_{\alpha}\rangle$ are the resulting *local* bath states—one for each grid point α used to cover the relevant subsystem configuration space—which are further written as

$$|\Phi_{\alpha}\rangle = |\phi_{\alpha}^1\rangle|\phi_{\alpha}^2\rangle\cdots|\phi_{\alpha}^F\rangle, \tag{2}$$

where F is the number of bath DOF. Here, $|\phi_{\alpha}^k\rangle$ are the bath single-particle functions, which are fully flexible in LTDH whereas in LCSA they are constrained to have a CS form ($|\phi_{\alpha}^k\rangle \equiv |z_{\alpha}^k\rangle$). [Here and in the following z^k is a *c* number which uniquely identifies the standard CS given by $|z^k\rangle = \exp(-|z^k|^2/2)\exp(z^k a_k^\dagger)|0\rangle$ where a_k is the lowering operator for the *k*th bath harmonic oscillator and $|0\rangle$ is its ground-state. See our previous paper (Ref. 46)]. With the help of the Dirac–Frenkel principle, the use of DVR states allows very simple equations of motion, as they always guarantee orthogonality between the configurations entering in Eq. (1), irrespective of the "shapes" of the local bath states, $|\Phi_{\alpha}\rangle$. In addition, if the CS approximation for the bath is introduced, they are also physically sound, in that they correspond to a Schrodinger–Langevin like equation for the system and pseudoclassical equations for the bath variables, containing both a classical and a quantum force.[46,47]

From the point of view of computational efficiency, there is no real need to use a DVR basis in place of any other orthogonal set. The system basis-set need not even be static, though in this case one has to consider the (small) additional effort required to compute the additional mean-fields and to evolve the basis functions in time. In this paper, we replace in Eq. (1) the DVR states with eigenstates of the subsystem Hamiltonian, as the latter lead to considerable simplification too. The purpose is to show that quite accurate results can be obtained by choosing a proper system basis when selecting the configurations to evolve. For LCSA this is true, in particular, without any additional empirical parameter which in Ref. 46 was added to remove numerical instabilities of the method. We further show that the resulting "energy-local" LTDH and LCSA (which we call eLTDH and eLCSA, respectively) provide very similar results, at least in the dissipative problems considered here. This means that the (local) CS approximation for the bath can be rather accurate, given that the bath is usually harmonic and the *ansatz* of Eqs. (1) and (2) introduces the main part of the important correlations between the system and the bath. As a whole, the results presented below show the importance of the system basis-set in expanding the wavefunction according to Eqs. (1) and (2). This is clearly the case because the quality of the approximation in Eq. (2), which is quite effective in reducing the computational cost of a full multiconfiguration expansion, does depend on the system set. In general, there is no set that works best for all typical problems at all times, and this leads directly to its variational optimization. This will be the subject of a forthcoming paper.

II. THEORY

Equations of motion for eLTDH/eLCSA can be obtained from the Dirac–Frenkel variational principle and read exactly as those of LTDH/LCSA (see, e.g., Refs. 45 and 46), the only difference being the replacement of DVR states with system eigenstates. This means that differences arise only when explicitly writing matrix elements of the chosen Hamiltonian; in particular, notice that previous LTDH/LCSA made use of the DVR approximation in representing local system operators, i.e., $f_{\alpha\beta} \approx \delta_{\alpha\beta}f(x_{\alpha})$, which can no longer be used in the present context. The equation for the amplitude coefficients C_{α} reads as

$$i\hbar\dot{C}_{\alpha} = \sum_{\beta}\langle\xi_{\alpha}\Phi_{\alpha}|H|\xi_{\beta}\Phi_{\beta}\rangle C_{\beta} + v_{\alpha}^{\text{gauge}}C_{\alpha}, \tag{3}$$

where $v_{\alpha}^{\text{gauge}}$ is a *gauge* potential related to the normalization constraints of the bath single-particle functions, $v_{\alpha}^{\text{gauge}} = -i\hbar\sum_{k=1}^{F}\langle\phi_{\alpha}^k|\dot{\phi}_{\alpha}^k\rangle$. In eLTDH the constraints $\hbar\langle\phi_{\alpha}^k|\dot{\phi}_{\alpha}^k\rangle = -ig_{\alpha}^k$ ($g_{\alpha}^k \in \mathbb{R}$) can be chosen arbitrarily (though we simply put $g_{\alpha}^k \equiv 0$ in the following), whereas in eLCSA, as in LCSA, we fix for convenience the phase of coherent states and use the equation

$$\langle z_{\alpha}^k|\dot{z}_{\alpha}^k\rangle = i\,\text{Im}(z_{\alpha}^{k*}\dot{z}_{\alpha}^k),$$

which holds for standard CSs. The equations of motion for the bath single-particle functions read as

$$i\hbar(1 - P_{\alpha}^k)C_{\alpha}|\dot{\phi}_{\alpha}^k\rangle = (1 - P_{\alpha}^k)\sum_{\beta}C_{\beta}H_{\alpha\beta}^k|\phi_{\beta}^k\rangle, \tag{4}$$

where $H_{\alpha\beta}^k = \langle \xi_\alpha \Phi_\alpha^k | H | \xi_\beta \Phi_\beta^k \rangle$ is the mean-field Hamiltonian matrix for the kth degree of freedom, $|\Phi_\alpha^k\rangle = \langle \phi_\alpha^k | \Phi_\alpha \rangle$ is the kth single-hole bath vector corresponding to the α subsystem state, and $P_\alpha^k = |\phi_\alpha^k\rangle \langle \phi_\alpha^k |$ is a projector onto the occupied space of the kth DOF. Notice that in the equation above $i\hbar P_\alpha^k |\dot\phi_\alpha^k\rangle = g_\alpha^k |\phi_\alpha^k\rangle$, i.e., Eq. (4) represents an explicit equation for the time-derivative $|\dot\phi_\alpha^k\rangle$. The eLCSA version of these equations may be obtained directly from Eq. (4) by observing that in this case the allowed variations are

$$\delta |z^k{}_\alpha\rangle = \frac{\partial |z^k{}_\alpha\rangle}{\partial x_\alpha^k} \delta x_\alpha^k + \frac{\partial |z^k{}_\alpha\rangle}{\partial y_\alpha^k} \delta y_\alpha^k,$$

where $x_\alpha^k = \mathrm{Re}\, z_\alpha^k$ and $y_\alpha^k = \mathrm{Im}\, z_\alpha^k$. Using simple manipulations[46] they read as

$$i\hbar C_\alpha \dot z_\alpha^k = \langle z_\alpha^k | \left(- z_\alpha^k + a_k \right) \sum_\beta C_\beta H_{\alpha\beta}^k |z_\beta^k\rangle, \qquad (5)$$

where a_k is the harmonic-oscillator (HO) lowering operator of the kth degree of freedom.

Next, we introduce the typical system-bath Hamiltonian which is used to model dissipative dynamics,

$$H = H^{\mathrm{sys}} + H^{\mathrm{env}},$$

$$H^{\mathrm{env}} = - \sum_{k=1}^F \left(\lambda_k^\dagger a_k + \lambda_k a_k^\dagger \right) + \sum_{k=1}^F \hbar\omega_k a_k^\dagger a_k,$$

where H^{sys} is the subsystem Hamiltonian, and H^{env} is the "environment" Hamiltonian which is here written as a sum of an interaction term H^{int} (the first term on the last line) and a bath Hamiltonian H^{bath} (the last term). The subsystem-bath coupling is assumed to be linear in the bath coordinates but arbitrary in the subsystem coordinates; $a_k^\dagger, a_k$ are the usual HO raising/lowering operators. With this Hamiltonian Eq. (3) becomes

$$i\hbar \dot C_\alpha = \left(\epsilon_\alpha + v_\alpha^{\mathrm{bath}} + v_\alpha^{\mathrm{gauge}} \right) C_\alpha + \sum_\beta \langle \xi_\alpha \Phi_\alpha | H^{\mathrm{int}} | \xi_\beta \Phi_\beta \rangle C_\beta,$$

where ϵ_α is the αth system energy eigenstate, $H^{\mathrm{sys}} |\xi_\alpha\rangle = \epsilon_\alpha |\xi_\alpha\rangle$, and $v_\alpha^{\mathrm{bath}} = \langle \Phi_\alpha | H^{\mathrm{bath}} | \Phi_\alpha \rangle$. The last term on the right-hand-side is the only one requiring off-diagonal elements between configurations,

$$\langle \xi_\alpha \Phi_\alpha | H^{\mathrm{int}} | \xi_\beta \Phi_\beta \rangle = - \sum_{k=1}^F \left\{ (\lambda_k)_{\beta\alpha}^* \langle \Phi_\alpha | a_k | \Phi_\beta \rangle + (\lambda_k)_{\alpha\beta} \langle \Phi_\beta | a_k | \Phi_\alpha \rangle^* \right\},$$

where $(\lambda_k)_{\alpha\beta} = \langle \xi_\alpha | \lambda_k | \xi_\beta \rangle$. It is clear from this equation that the "energy-local" bath states $|\Phi_\alpha\rangle$ provide a coupling for the C_α's (and therefore for the populations of the system energy levels, $n_\alpha = |C_\alpha|^2$) only if they have a different excitation level (number of phonons) in at least one bath oscillator. On the other hand, simplifications also occur in Eq. (4), since $H_{\alpha\beta}^k$

now reads as

$$H_{\alpha\beta}^k = \delta_{\alpha\beta} \left[\epsilon_\alpha + \sum_{k'=1}^{k'\neq k} \hbar\omega_{k'} n_{k'}^\alpha + \hbar\omega_k a_k^\dagger a_k \right]$$
$$- \left[(\lambda_k)_{\beta\alpha}^* a_k + (\lambda_k)_{\alpha\beta} a_k^\dagger \right] O_{\alpha\beta}^k$$
$$- \sum_{k'=1}^{k'\neq k} \left[(\lambda_{k'})_{\beta\alpha}^* \Gamma_{\alpha\beta}^{k'} + (\lambda_{k'})_{\alpha\beta} \Gamma_{\beta\alpha}^{k'*} \right] O_{\alpha\beta}^{kk'},$$

where n_k^α is an average number of phonons in the kth oscillator, $n_k^\alpha = \langle \phi_\alpha^k | a_k^\dagger a_k | \phi_\alpha^k \rangle$, $\Gamma_{\alpha\beta}^k$ is defined similarly as $\Gamma_{\alpha\beta}^k = \langle \phi_\alpha^k | a_k | \phi_\beta^k \rangle$, $O_{\alpha\beta}^k$ is an overlap matrix element between single-hole vectors $O_{\alpha\beta}^k = \langle \Phi_\alpha^k | \Phi_\beta^k \rangle = \prod_{i\neq k} \langle \phi_\alpha^i | \phi_\beta^i \rangle$, and $O_{\alpha\beta}^{kk'}$ is defined analogously for double-hole vectors, $O_{\alpha\beta}^{kk'} = \langle \Phi_\alpha^{kk'} | \Phi_\beta^{kk'} \rangle = \prod_{i\neq k,k'} \langle \phi_\alpha^i | \phi_\beta^i \rangle$.

Considerable simplification occurs in the LCSA case, using the well-known properties of CSs. For instance, $\langle \Phi_\alpha | a_k | \Phi_\beta \rangle = z_\beta^k O_{\alpha\beta}$, $n_k^\alpha = |z_\alpha^k|^2$, and $\Gamma_{\alpha\beta}^k = z_\beta^k \langle z_\alpha^k | z_\beta^k \rangle$, etc. The overlap matrix elements between CSs are also analytically available,

$$\langle z | w \rangle = e^{z^* w - (|z|^2/2) - (|w|^2/2)} = e^{-(|z-w|^2/2) + i\,\mathrm{Im}\, z^* w}$$

More generally, the equations of motion for CSs can be obtained from Eq. (5) by using[47]

$$a_k H^{\mathrm{env}} = H^{\mathrm{env}} a_k + \left[a_k, H^{\mathrm{env}} \right] = H^{\mathrm{env}} a_k + \frac{\partial H_{\mathrm{ord}}^{\mathrm{env}}}{\partial a_k^\dagger},$$

where $H_{\mathrm{ord}}^{\mathrm{env}}$ is the environment Hamiltonian with the phonon creation/annihilation operators ordered in the usual way, i.e., all powers of $a_k^\dagger$'s on the left of all a_k's (see, e.g., Refs. 48 and 49). For the above Hamiltonian,

$$\frac{\partial H_{\mathrm{ord}}^{\mathrm{env}}}{\partial a_k^\dagger} = \hbar\omega_k a_k - \lambda_k,$$

and the final result is

$$i\hbar C_\alpha \dot z_\alpha^k = \hbar\omega_k z_\alpha^k C_\alpha - \sum_\beta \Lambda_{\alpha\beta} O_{\alpha\beta} (z_\beta^k - z_\alpha^k) C_\beta$$
$$- \sum_\beta (\lambda_k)_{\alpha\beta} O_{\alpha\beta} C_\beta,$$

where $\Lambda_{\alpha\beta} = \sum_k (\lambda_k)_{\beta\alpha}^* z_\beta^k + (\lambda_k)_{\alpha\beta} z_\alpha^{k*}$; from this the CSs time derivatives entering the *gauge* potential of Eq. (3) can be explicitly removed.

Before leaving this section it is worth noting that the parametrization of the wavefunction as defined by the LTDH/LCSA *ansatz* (and the modified counterparts discussed in this paper) is *singular* when $C_\alpha = 0$, since in that case the corresponding bath configuration $|\Phi_\alpha\rangle$ can be chosen arbitrarily. This does *not* affect the results of Eq. (4), whose solution is needed only for $C_\alpha \neq 0$, rather those of Eq. (3) where $\dot C_\alpha$ would then depend on the *arbitrary* configuration $|\Phi_\alpha\rangle$. Our experience tells us that this is not a real problem, since the main results do not depend on such choice. More importantly, it is worth noting that by combining Eqs. (3) and (4) the following expression for the time-derivative of the total

wavefunction can be obtained:

$$i\hbar \,|\dot{\Psi}\rangle = \sum_{\alpha\beta} |\xi_\alpha \Phi_\alpha\rangle \, H_{\alpha\beta} C_\beta$$

$$+ \sum_{k=1}^{F} \sum_{\alpha,\beta} |\xi_\alpha \Phi_\alpha^k\rangle \left(1 - P_\alpha^k\right) H_{\alpha\beta}^k \,|\phi_\beta^k\rangle \, C_\beta.$$

With the Hamiltonian above it is not hard to show that this time-derivative is the same as the *exact* one, $i\hbar \,|\dot{\Psi}^{\text{exact}}\rangle = H\,|\Psi\rangle$, for a number of (initial) vectors $|\Psi\rangle$, for instance those of the form $|\xi\rangle\,|n\rangle$ where $|\xi\rangle$ is an arbitrary system state and $|n\rangle = |n_1, \ldots, n_k, \ldots, n_F\rangle$ is a bath eigenstate (similarly for bath CSs and LCSA). Thus, in such situations the correct short-time behavior is guaranteed by the LTDH/LCSA *ansatz*.

III. THE MODEL

In Sec. IV we use the eLTDH/eLCSA methods introduced above for solving a number of model problems, and compare the results with those of numerically exact MCTDH calculations. The model has been described in previous papers[45, 46, 50] and will be only sketched here for completeness. It consists of a Morse oscillator (with coordinate x and momentum p) coupled to a number F of bath oscillators,

$$H = \frac{p^2}{2m} + v(x) - f(x) \sum_{k=1}^{F} c_k q_k$$

$$+ \sum_{k=1}^{F} \frac{p_k^2}{2m_k} + \frac{m_k \omega_k^2 q_k^2}{2}. \qquad (6)$$

The bath frequencies ω_k and the coupling coefficients c_k are chosen in such a way to sample a given spectral density $J(\omega)$, which is the only quantity of interest for the subsystem dynamics (see Refs. 50–52 for some recent attempt in exploiting this property). Thus the harmonic oscillator bath is here meant to model fluctuations in and dissipation to a given, arbitrarly complex environment and does not necessarily correspond to a real system. $J(\omega)$ is a real, odd function defined by the real part ($\gamma'(\omega)$) of the frequency-dependent memory-kernel $\gamma(\omega)$,

$$J(\omega) = m\omega\gamma'(\omega).$$

The memory-kernel $\gamma(t)$ (the Fourier transform of $\gamma(\omega)$) enters the generalized Langevin equation, here written for state-dependent friction:

$$m\ddot{x} = -\tilde{v}'(x)$$

$$+ f'(x) \left(\xi(t) - m \int_{t_0}^{\infty} \gamma(t-\tau) f'(x(\tau)) \dot{x}(\tau) \, d\tau \right). \qquad (7)$$

Knowledge of $J(\omega)$ suffices to determine[3] $\gamma(\omega)$ by virtue of the Kramers–Kronig relations, as well as the correlation function of the random force $\xi(t)$ by virtue of the fluctuation-dissipation theorem

$$\langle \xi(t)\xi(t') \rangle = m k_B T \gamma(|t - t'|).$$

This completely specifies the stationary *Gaussian* process $\xi(t)$. For the microscopic model of Eq. (6), which is known to lead to Eq. (7) in the continuum limit, $J(\omega)$ reads for $\omega > 0$ as

$$J(\omega) = \frac{\pi}{2} \sum_{k} \frac{c_k^2}{m_k \omega_k} \delta(\omega - \omega_k).$$

For a set of evenly spaced frequencies, $\omega_k = k\Delta\omega$, $J(\omega) \approx \pi c^2(\omega)/2m_\omega\omega\Delta\omega$, and one gets the coupling coefficients which sample the spectral density $J(\omega)$,

$$c_k = \left(\frac{2m_k \omega_k \Delta\omega J(\omega_k)}{\pi} \right)^{1/2}.$$

The frequency spacing $\Delta\omega$ sets the Poincaré recurrence time, $T_{\text{rec}} = 2\pi/\Delta\omega$, which must be larger than any time of physical interest. The masses of the bath oscillators, on the other hand, do not play any role in the dynamics, as it is clear by rewriting the above Hamiltonian in terms of the (adimensional) operators $a_k, a_k^\dagger$. In the following we use a truncated Ohmic spectral density, $J(\omega) = m\gamma\omega$ for $\omega \leq \omega_c = F\Delta\omega$ and $J(\omega) = 0$ for $\omega > \omega_c$, which describes a subsystem dynamics with relaxation time γ^{-1} which is Markovian for times greater than $\sim \omega_c^{-1}$; thus, even in this simple model, if $\gamma \gtrsim \omega_c$ the dynamics is non-Markovian in the interesting time-window.

The potential $\tilde{v}(x)$ entering in Eq. (7) is the renormalized subsystem potential

$$\tilde{v}(x) = v(x) - \frac{1}{2}[f(x)]^2 \sum_{k} \frac{c_k^2}{m_k \omega_k^2},$$

as results from the coupling-induced renormalization of the system dynamics. The renormalization correction is usually eliminated by adding to Eq. (6) a counterterm, but since we are going to compare results with those resulting from numerically exact calculations using the same Hamiltonian there is no real need to add this term for such purpose. Notice that with our model spectral function the renormalized potential reads as

$$\tilde{v}(x) = v(x) - \frac{m\gamma\omega_c}{\pi}[f(x)]^2,$$

and it is clear that for high cutoff frequencies and/or γ dynamical instabilities appear. In particular, for bound potentials, say $v(x) \to D_e$ for $x \to \infty$, the limit of $f(x)$ may be important in that respect, too. We choose the coupling function as in previous works,[45, 46, 50] namely,

$$f(x) = \frac{1 - e^{-\alpha x}}{\alpha},$$

where α is the frequency parameter of the Morse potential

$$v(x) = D_e(1 - e^{-\alpha x})^2.$$

This function reduces to $f(x) \sim x$ close to the equilibrium position of the Morse oscillator, but tends to a finite value when $x \to \infty$. With this choice, the renormalized potential above is still of a Morse type, with a corresponding $\tilde{D}_e = D_e - m\gamma\omega_f/\pi\alpha^2$.

In the following, the subsystem is meant to represent a hydrogen atom chemisorbed on a surface. A standard,

Colbert–Miller DVR set[53] was introduced as a primitive grid to represent the subsystem Hamiltonian operator, which was then diagonalized to obtain the energy eigenstates used for eLTDH/eLCSA. The Morse potential parameters are set to $D_e = 1.55$ eV, $\alpha = 1.238\, a_0^{-1}$, and the bath cutoff frequency is fixed to be twice the corresponding Morse oscillator frequency ($T_c = 2\pi/\omega_c \approx 8$ fs). The bath is discretized with 80 bath oscillators, in such a way that the recurrence time is large enough ($T_{\text{rec}} \approx 610$ fs) for describing dissipation. Additional tests with 120 modes (and the same ω_c) showed that the number of bath oscillators does not play any role, for $t < T_{\text{rec}}$ above, at *any* level of description.

IV. RESULTS

A. Small amplitude motion

First we consider the damped motion of the Morse oscillator initially displaced from its equilibrium position. The initial wavefunction is of product form $|\psi\rangle |\Phi\rangle$, $|\psi\rangle$ being a Gaussian wavepacket centered in x_0 and $|\Phi\rangle$ the ground-state of the interacting bath at a sharply defined subsystem position x_0. The system starts to oscillate and transfers energy to the bath, though more efficiently when it reaches the inner turning point, i.e., where the interaction with the bath is strongest.

The results of our calculations are reported in Fig. 1 where we show the behavior of the average position $\langle x \rangle$ and average system energy $E^{\text{sys}} = \langle H^{\text{sys}} \rangle$ for three different values of the relaxation time ($\gamma^{-1} = 8, 50,$ and 200 fs); note, in particular, that the energy decay is not Markovian for the strongest coupling considered. It is clear from Fig. 1 that both eLTDH and eLCSA perform rather well and correctly reproduce the numerically exact MCTDH results. This is true (more or less to the same extent) for all the coupling strengths considered. This is even more impressive if the very small computational cost of the two methods is taken into account: for instance, the longest eLCSA calculations in Fig. 1 took
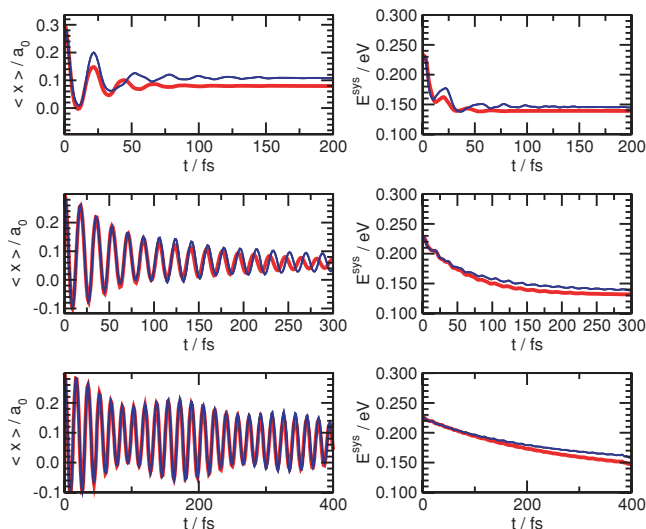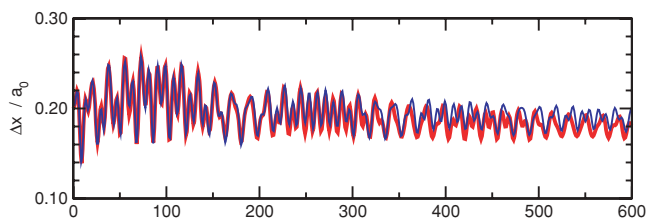

FIG. 2. Width of the wavepacket along x for $\gamma^{-1} = 200$ fs. Lines as in Fig. 1.

about 2–3 min on a standard PC. The quality of the results is not limited to the most averaged quantities, as can be seen in Fig. 2 where we plot for instance the behaviour of the width Δx of the wavepacket along the subsystem coordinate, $\Delta x^2 = \langle x^2 - \langle x \rangle^2 \rangle$.

B. Sticking dynamics

In modeling sticking of an atom to a cold surface (actually a $T = 0$ K surface) we use the same Hamiltonian as above but different initial conditions. The bath, then, is meant to represent a set of surface phonons, even though the chosen Ohmic spectral density is far from being realistic for such a process. The initial state of the system is chosen to be a Gaussian wavepacket localized far from the surface (i.e., at a large x) and with momentum directed towards it, and the bath is in its ground-state. As the projectile gets closer to the surface, where the system-bath coupling is not constant, energy is transferred to the bath and "vibrational" relaxation occurs. The projectile wavepacket splits into two components, one of which is (inelastically) reflected by the surface and the other gets stuck to it. Because of that, this simple process cannot be described within the simple mean-field theory (TDSCF).

For this problem we considered different values of the coupling strength (described by the relaxation time γ^{-1} in our Ohmic model) and different collision energies, and in each case looked at the energy transfer by monitoring the system and the interaction energy during the dynamics. The sticking coefficient was obtained as the mean value of the projector onto bound states at a time sufficiently long that the inelastically scattered wavepacket already left the interaction region. This poses severe limitations at very low collision energies—the deep quantum regime—where (very) large baths are needed to get rid of the recurrence problem, and a time-energy mapping of the wavepacket dynamics is mandatory. As this would be much beyond the purpose of the present paper, we limit ourselves to reasonably high energies where numerically exact MCTDH calculations are still feasible and physically meaningful, and report the results in terms of *average* collision energy E_{coll} of initial wavepackets with $\Delta E \ll E_{\text{coll}}$. Notice also that the dynamics was followed for reasonably small times only, i.e., sufficiently long to observe sticking but not enough to resolve relaxation of the trapped component to the final, ground vibrational state.

Calculations were performed by discretizing the continuous energy spectrum, i.e., employing the energy eigenstates obtained with a primitive DVR grid large enough to
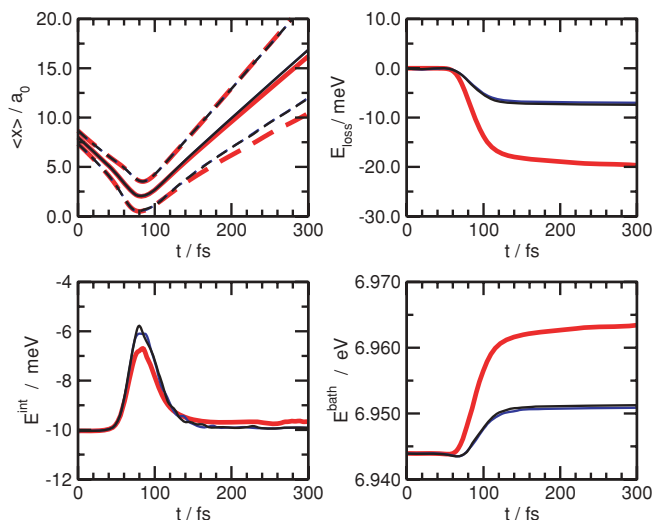

FIG. 1. Small amplitude motion for different relaxation times ($\gamma^{-1} = 8, 50, 200$ fs from top to bottom): behavior of the average position (left) and system energy (right). Thick red lines for MCTDH results, black and blue lines for eLTDH and eLCSA.

FIG. 3. Sticking dynamics for $\gamma^{-1} = 1000$ fs and $E_{coll} = 75$ meV. Top left panel: average system position (solid lines) plus/minus one standard deviation (dashed lines). Top right: (corrected) system energy loss. Bottom panels: interaction (left) and bath (right) energy. Thick red lines for MCTDH results, black and blue lines for LTDH and eLCSA, respectively.

contain the initial wavepacket and dense enough to represent the largest kinetic energy of interest, and convergence of results was checked against grid parameters and number of energy eigenstates included in the expansion. No complex absorbing potential was added at the grid edge since the chosen grids were large enough to converge the sticking probability before the edge-reflected component of the wavepacket could come back to the interaction region. Some of the results of such calculations are reported in Figs. 3–5. In Fig. 3 we report the average position $\langle x \rangle$, the average energy loss (defined to be $E_I^{sys}(t) - E_I^{sys}(0)$, where $E_I^{sys} = E^{sys} + 1/2 E^{int}$ is the "democratically corrected" system energy[50]) and the average interaction energy as obtained from MCTDH, eLTDH, and eLCSA calculations, for a collision energy $E_{coll} = 75$ meV and a relaxation time $\gamma^{-1} = 1000$ fs. We see that the agreement between exact and approximate calculations is not as good as in Sec. IV A. This is particularly true for the aver-
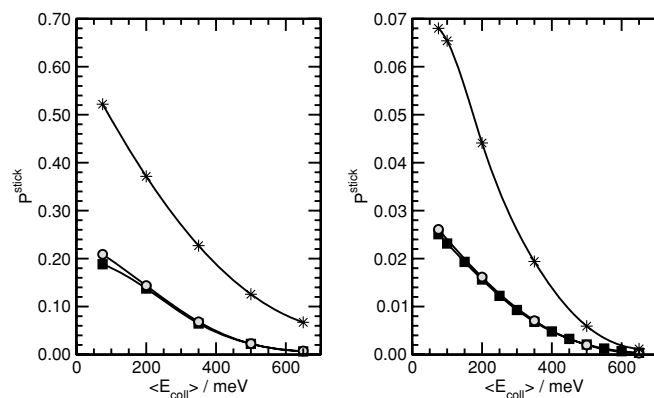

FIG. 4. Sticking coefficient for the gas-surface model described in the main text. Left and right panels for $\gamma^{-1} = 100$ and 1000 fs, respectively. Star symbols are for MCTDH results, circles for LTDH, and squares for eLCSA. Lines are guides for the eyes.
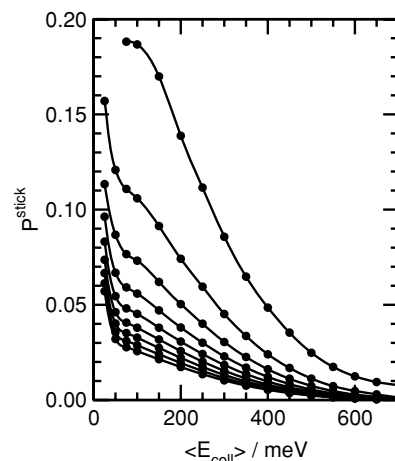

FIG. 5. The behavior of the sticking coefficient for several values of the relaxation time γ^{-1} in the range $100 - 1000$ fs (from top to bottom), as computed at the eLCSA level.

age energy loss which is always found lower than the exact one. This reflects on the sticking process itself, as the resulting sticking coefficient, shown in Fig. 4 for several collision energies, turns out to be slightly less than half the exact one. This is clearly a limit of the present *ansatz* which does introduce system-bath correlations (in contrast to TD-SCF) but is not able to "switch" to a more localized picture of the energy-transfer as relaxation proceeds. Such failure depends only weakly on the collision energy and the coupling strength, as it is evident from Fig. 4 where both a weak and a strong coupling case are reported (left and right panels for $\gamma^{-1} = 100$ and 1000 fs, respectively).

What is surprising is the close agreement between eLTDH and eLCSA results even in this not fully satisfactory case. This seems to exclude the lack of flexibility in the coherent-state description of local bath states. Indeed, original LCSA proved to be quite accurate in describing the dynamics, it only lacked sufficient numerical stability to be useful for extracting sticking coefficients.[47] In contrast, eLCSA results presented here (and analogously for eLTDH) are stable against any change in numerical and physical parameters, and can already be used for semiquantitative studies. Figure 5, for instance, reports the behavior of the sticking coefficient for the present model as obtained at the eLCSA level of theory; the whole set of calculations for filling the graph (all with 80 bath modes, large grids, long propagation times, etc.) requires a few hours with standard computational facilities.

V. DISCUSSION

We have shown in Sec. IV that reasonably good results can be obtained with eLTDH/eLCSA, at the same computational cost of the original LTDH/LCSA methods. In particular for LCSA the results have been obtained without the help of the additional "damping" parameter which was introduced in Ref. 46 to remove numerical instabilities of the method. Despite some interesting properties, indeed, the need for such a parameter is of course an undesirable feature of the method.

For instance, while in the case of the damped oscillations such a parameter allows one to get very accurate results and to remove the bath recurrence problem, in the sticking problem its presence, *alas*, causes the disappearance of sticking.[47] Therefore, the results obtained here for such problem, though giving only about half the exact sticking coefficient, are encouraging in that they suggest that there is still room for improvement, i.e., by properly choosing the system basis-set on which performing the selection of configurations one can get more accurate results without introducing numerical noise. Such optimal choice depends on time and therefore we are led to consider in a natural way the following "generalized" LTDH/LCSA *ansatz*:

$$|\Psi\rangle = \sum_\alpha C_\alpha |\psi_\alpha\rangle |\phi_\alpha^1\rangle \cdots |\phi_\alpha^k\rangle \cdots |\phi_\alpha^F\rangle,$$

where $\{C_\alpha, \psi_\alpha, \ldots, \phi_\alpha^k, \ldots\}$ are *all* dynamical variables (with ϕ_α^k replaced by simple *c*-numbers z_α^k in the LCSA case). The $\psi_\alpha(t)$'s would interpolate at any time t between the two "limiting" situations where the system basis-set is localized/delocalized in configuration space, i.e., the cases of LTDH/eLTDH discussed so far. The corresponding equations of motion for the ψ_α's are easily derived from the Dirac–Frenkel variational principle and will be discussed and solved in a forthcoming paper. Here we notice only that, even though they require some additional computational effort, the generalized (or fully time-dependent) LTDH/LCSA would be still and by far numerically advantageous with respect to fully multiconfiguration expansions. Indeed, they would preserve the power-law scaling (*linear* scaling for the model Hamiltonian above) with respect to the bath size and would correctly describe the important system-bath correlation, contrary, e.g., to simple TDSCF. In addition, the good agreement between the eLTDH and eLCSA results suggests that it is not even necessary to perform a full optimization of the bath single-particle-functions, and in that case the considerable saving of computational memory and time should allow us to easily treat thousands of bath DOFs as in the LCSA case.[46] If it turns out that the generalized methods are of such high quality as the present results suggest, larger dimensional *subsystems* can be managed by further expanding the ψ_α's in a MCTDH-fashion, thereby leading to a clean, physically motivated, easy-to-implement selection of configurations in a multiconfiguration expansion of the wavefunction of the whole system.

VI. SUMMARY

We have implemented and used a variant of the LTDH (also known as CC-TDSCF) and LCSA methods in which the DVR subsystem states are replaced by energy eigenstates. The methods have been applied to some dissipative problems and the results compared with those of numerically exact MCTDH calculations. Given their low computational cost and the remaining room for improvements the results suggest that in the near future realistic system-bath problems might be addressed quantitatively with present-day computational facilities.

[1]K. Blum, *Density Matrix Theory and Applications* (Plenum, New York, 1996).
[2]H.-P. Breuer and F. Petruccione, *The Theory of Open Quantum Systems* (Oxford, Oxford, 2002).
[3]U. Weiss, *Quantum Dissipative Systems*, 3rd ed. (World Scientific, Singapore, 2008).
[4]M. H. Beck, A. Jackle, G. A. Worth, and H.-D. Meyer, Phys. Rep. **324**, 1 (2000).
[5]*Multidimensional Quantum Dynamics: MCTDH Theory and Applications*, edited by H.-D. Meyer, F. Gatti, and G. A. Worth (Wiley-VCH, 2009).
[6]A. D. Hammerich, U. Manthe, R. Kosloff, H.-D. Meyer, and L. S. Cederbaum, J. Chem. Phys. **101**, 5623 (1994).
[7]L. Liu, J. Y. Fang, and H. Guo, J. Chem. Phys. **102**, 2404 (1995).
[8]B. Pouilly, M. Monnerville, F. Gatti, and H.-D. Meyer, J. Chem. Phys. **122**, 184313 (2005).
[9]S. Woittequand, C. Toubin, B. Pouilly, M. Monnerville, S. Briquez, and H.-D. Meyer, Chem. Phys. Lett. **406**, 202 (2005).
[10]H. Köppel, M. Döscher, I. Baldea, H.-D. Meyer, and P. G. Szalay, J. Chem. Phys. **117**, 2657 (2002).
[11]E. V. Gromov, A. B. Trofimov, N. M. Vitkovskaya, H. Köppel, J. Schirmer, H.-D. Meyer, and L. S. Cederbaum, J. Chem. Phys. **121**, 4585 (2004).
[12]A. Markmann, G. A. Worth, S. Mahapatra, H.-D. Meyer, H. Köppel, and L. S. Cederbaum, J. Chem. Phys. **123**, 204310 (2005).
[13]J. Y. Fang and H. Guo, J. Chem. Phys. **102**, 1944 (1995).
[14]C. Meier and U. Manthe, J. Chem. Phys. **115**, 5477 (2001).
[15]F. Matzkies and U. Manthe, J. Chem. Phys. **110**, 88 (1999).
[16]A. Jäckle, M. Heitz, and H.-D. Meyer, J. Chem. Phys. **110**, 241 (1999).
[17]S. Sukiasyan and H.-D. Meyer, J. Chem. Phys. **116**, 10641 (2002).
[18]F. Huarte-Larrañaga and U. Manthe, J. Chem. Phys. **118**, 8261 (2003).
[19]G. Nyman, R. van Harrevelt, and U. Manthe, J. Phys. Chem. A **111**, 10331 (2007).
[20]J. Y. Fang and H. Guo, Chem. Phys. Lett. **235**, 341 (1995).
[21]M. Ehara, H.-D. Meyer, and L. S. Cederbaum, J. Chem. Phys. **105**, 8865 (1996).
[22]R. Milot and A. P. J. Jansen, J. Chem. Phys. **109**, 1966 (1998).
[23]M. Heitz and H.-D. Meyer, J. Chem. Phys. **114**, 1382 (2001).
[24]R. van Harrevelt, K. Honkala, J. K. Nørskov, and U. Manthe, J. Chem. Phys. **122**, 234702 (2005).
[25]C. Crespos, H.-D. Meyer, R. C. Mowrey, and G. J. Kroes, J. Chem. Phys. **124**, 074706 (2006).
[26]*Heidelberg's mctdh homepage*, see http://www.pci.uni-heidelberg.de/cms/mctdh.html.
[27]M. Nest and H.-D. Meyer, J. Chem. Phys. **119**, 24 (2003).
[28]I. Burghardt, M. Nest, and G. A. Worth, J. Chem. Phys. **119**, 5364 (2003).
[29]H. Wang and M. Thoss, J. Chem. Phys. **119**, 1289 (2003).
[30]U. Manthe, J. Chem. Phys. **128**, 164116 (2008).
[31]U. Manthe, J. Chem. Phys. **130**, 054109 (2009).
[32]H. Wang and M. Thoss, in *Multidimensional Quantum Dynamics: MCTDH Theory and Applications*, edited by H.-D. Meyer, F. Gatti, and G. A. Worth (Wiley-VCH, Weinheim, 2009), Chap. 14.
[33]H. Wang and M. Thoss, J. Chem. Phys. **124**, 034114 (2006).
[34]H. Wang, D. Skinner, and M. Thoss, J. Chem. Phys. **125**, 174502 (2006).
[35]I. Kondov, M. Thoss, and H. Wang, J. Phys. Chem. A **110**, 1364 (2006).
[36]I. Craig, M. Thoss, and H. Wang, J. Chem. Phys. **127**, 144503 (2007).
[37]I. Burghardt, H.-D. Meyer, and L. S. Cederbaum, J. Chem. Phys. **111**, 2927 (1999).
[38]G. A. Worth and I. Burghardt, Chem. Phys. Lett. **368**, 502 (2003).
[39]G. A. Worth, M. A. Robb, and I. Burghardt, Faraday Discuss. **127**, 307 (2004).
[40]D. V. Shalashilin and M. S. Child, J. Chem. Phys. **113**, 10028 (2000).
[41]D. V. Shalashilin and M. S. Child, J. Chem. Phys. **115**, 5367 (2001).
[42]G. A. Worth, J. Chem. Phys. **112**, 8322 (2000).
[43]D. H. Zhang, W. Bao, M. Yang, and S.-Y. Lee, J. Chem. Phys. **122**, 091101 (2005).
[44]L. Zhang, S.-Y. Lee, and D. H. Zhang, J. Phys. Chem. A **110**, 5513 (2006).
[45]S. López-López and M. Nest, J. Chem. Phys. **132**, 104103 (2010).

[46]R. Martinazzo, M. Nest, P. Saalfrank, and G. F. Tantardini, J. Chem. Phys. **125**, 194102 (2006).

[47]R. Martinazzo, I. Burghardt, F. Martelli, and M. Nest, in *Multidimensional Quantum Dynamics With Trajectories*, edited by D. V. Shalashilin and M. P. de Miranda (University of Leeds, Leeds, 2009).

[48]J. R. Klauder and B. S. Skagerstam, *Coherent States: Applications in Physics and Mathematical Physics* (World Scientific, Singapore, 1985).

[49]C. W. Gardiner, *Quantum Noise* (Springer-Verlag, Berlin, 1991).

[50]K. H. Hughes, C. D. Christ, and I. Burghardt, J. Chem. Phys. **131**, 024109 (2009).

[51]K. H. Hughes, C. D. Christ, and I. Burghardt, J. Chem. Phys. **131**, 124108 (2009).

[52]R. Martinazzo, K. Hughes, F. Martelli, and I. Burghardt, Chem. Phys. **377**, 21 (2010).

[53]D. T. Colbert and W. H. Miller, J. Chem. Phys. **96**, 1982 (1992).